Rippling Instability of a Collapsing Bubble

Rava da Silveira*, Sahraoui Chaieb† and L. Mahadevan†
*Department of Physics, †Department of Mechanical Engineering
Massachusetts Institute of Technology, 77 Mass Ave., Cambridge, MA 02139, U.S.A.

The rippling instability of a liquid sheet was first observed by Debrégeas, de Gennes, and Brochard-Wyart [Science 279, 1704 (1998)] on a hemispherical bubble resting on a free surface. Unlike a soap bubble, it collapses under its own weight while bursting, and folds into a wavy structure which breaks the original axisymmetry. In fact, this effect occurs for both purely elastic and purely viscous (liquid) sheets, and an analogy can be made between the two mechanisms. We present a theory for the onset of the instability in both cases, in which the growth of the corrugation out of an inextensible initial condition is governed by the competition between gravitational and bending (shearing) forces. The instability occurs for a range of densities, stiffnesses (viscosities), and sizes, a result which arises less from dynamics than from geometry, suggesting a wide validity. We further obtain a quantitative expression for the number of ripples. Finally, we present the results of experiments, which are consistent with our predictions.

Every day, nature surprises us with structures and patterns of such beauty as to fill the scientist with wonder and the artist with envy. In the present paper, we address an instability which turns a uniform, smooth, liquid bubble into a striking wrinkled structure. The rippling of a deflating bubble was first observed by Debrégeas, de Gennes, and Brochard-Wyart [1]. In their experiment, 0.1 to 10 cm^3 of air injected in a highly viscous liquid ($\eta \sim 10^3$ Pa·s) rises to the free surface, imprisoned in a hemispherical bubble of thickness $e \sim 1 - 10$ μm. If the latter is perforated at its apex by a needle, a circular opening expands exponentially at first. After about 30 ms, the retraction slows down to a steady state. In the meantime, the air flow through the hole equilibrates the pressure difference, allowing the bubble to collapse under its own weight. As it deflates, an *instability* appears: the fluid sheet folds into a wavy structure, with radial ripples that break the original axisymmetry. In the absence of a detailed theory, Ref. [1] proposes a scaling estimate for the number of ripples $n^* \sim (\mu g R^3/K)^{1/2}$, where μ is the mass of the film per unit area, g the gravitational acceleration, R the radius of the hole, and K the effective bending rigidity of the sheet which was assumed to be elastic during the early stages of the rippling. Viscous flows eventually cause the corrugation to decay, as the hole retracts towards the thicker edge of the bubble.

The rippling results from the competition between compression, bending, and gravity. Each fluid element tends to fall under its own weight, but experiences a viscous resistance from its neighborhood. If the bubble were to collapse in a uniform, symmetric way, it would occupy a progressively reduced area, leading to an in-plane compression which would require forces that far exceed the scale set by gravity. Instead, the film deforms in a nearly inextensional fashion by undergoing pure bending almost everywhere. In terms of dynamics, this argument may be restated as follows; for a given (gravitational) force, the relative time scale associated with stretching is much larger than that for bending, and the surface therefore prefers to corrugate on short times, before eventually relaxing into a uniform, thicker membrane. We note that this is valid only for creeping flows; the instability does not occur in the bursting of low viscosity films such as soap bubbles, owing to the rapidity of the retraction.

This instability is reminiscent of buckling phenomena in slender elastic bodies [2]. In fact, creeping flows of liquid filaments and sheets may also lead to buckling (a striking everyday example being the coiling of a stream of honey when it reaches a toast [3,4]), an analogy we shall elucidate and exploit. For an elastic rod, buckling occurs at the longest possible wavelength in order to minimize the bending energy. In the bubble problem, however, gravity plays a distinctive role in determining the configuration. Though bending still favors large scale deformations, the gravitational energy is minimized for an almost flat sheet with as many tiny ripples as possible, and the optimal wavelength results from a compromise between the two.

The rippling instability corresponds to the growth of the most favorable perturbation, transforming an axisymmetric initial condition into a corrugated pattern of a given wavelength. Although the bubble has the geometry of a sphere before collapsing, it is quite flattened by the time the ripples appear. For simplicity, we consider the unperturbed configuration to be a shallow cone, of slope $\alpha \ll 1$, described by its height above the surface,

$$h = \alpha (\rho_0 - \rho), \qquad (1)$$

where ρ is the cylindrical radial coordinate and ρ_0 the radius of the base (Fig. 1(a)). As a further simplification, we do not incorporate the full bursting dynamics and corresponding viscous flows in our analysis, but carry it out with a specific hole size, which enters the theory as a parameter R. Once the hole grows steadily, the rate of retraction of the liquid film is given by the balance of viscous stress and surface tension ($\sigma \approx 20$ mN/m), resulting in a constant velocity $v \sim \sigma/\eta$. It thus takes a time $\tau \sim \eta e/\sigma$ for the opening radius to increase by e. In this time, the liquid acquires a velocity $V \sim g\tau$ due to gravity, larger than v by a factor $V/v \sim 10^7$. Even if the liquid is viscoelastic, so that the retraction velocity is enhanced by a factor R/e ($\sim 10-10^4$) [5,1], the hole radius remains essentially constant while the instability occurs.

To allow for the rippling of the surface, we perturb our truncated cone, without any loss of generality, as

$$h+\delta h = \alpha(\rho_0-\rho) - \delta\alpha(\rho) + \sum_{n\geq 1}\delta\beta_n(\rho)\cos(n\theta), \qquad (2)$$

where θ is the azimuthal angle. In the case of a thin elastic sheet loaded by its own weight, the two primary modes of deformation are in-plane stretching and out-of-plane bending. If the scale of the deformation is of $\mathcal{O}(l)$, the bending forces are proportional to Ye^3/l, while the stretching forces are proportional to Yel [6]. Their ratio scales as $(e/l)^2$, so that for a given external force, here due to gravity, inextensional deformations are greatly preferred. For a thin, very viscous sheet, the primary modes of deformation are also bending and stretching (shearing) ones. Here however, the forces result from velocity gradients in the sheet. For deformations (of the bubble) of $\mathcal{O}(l)$, the ratio of the viscous forces [7,8] due to bending, $(\eta e^3/l^2)\,dl/dt$, to those associated with stretching, $(\eta e)\,dl/dt$, is $(e/l)^2$, as before, largely favoring inextensional deformations if $e \ll l \approx \rho_0/n^*$. (This condition is satisfied if the selected number of ripples n^* is small compared to 10^3, which is the case as we shall see later). Equivalently, for a given loading, the time scale corresponding to bending is smaller than that for stretching by a factor $(e/l)^2$. Thus, at the onset of the instability we may neglect perturbations that involve stretching, both for the elastic and the viscous sheet. More specifically, we require (i) a vanishing Gauss curvature [9], leading to a developable surface, so that

$$\delta\alpha(\rho) = \delta\alpha \times (c-\rho), \quad \delta\beta_n(\rho) = \delta\beta_n \times \rho \qquad (3)$$

(where $\delta\alpha$, $\delta\beta_n$, and c are constants); (ii) no in-plane strains [9], yielding

$$\sum_{n\geq 1}(1+n^2)(\delta\beta_n)^2 = 4\alpha\delta\alpha. \qquad (4)$$

The perturbation thus consists of an axisymmetric flattening ($-\delta\alpha$) along with ripples of magnitude $\delta\beta_n$, analogous to the deformation of a tablecloth draping a circular table (Fig. 1(b)). We note that the inextensibility condition constrains the ripples to decrease in magnitude upon approaching the opening, in agreement with experimental observations. (The linear dependence of $\delta\alpha$ and $\delta\beta_n$ on ρ, though, remains to be checked.)

To complete the characterization of the problem, we have to specify boundary conditions for δh. As the bubble rests on a liquid substrate, its edge cannot sink, so that $\delta h(\rho=\rho_0)=0$. Clearly, this cannot be satisfied by the simple ansatz of Eq. (3), but requires one involving both bending and stretching. However, this stretching is restricted to a small region near the edge [6,10], so that the inextensional assumption holds in the bulk, along with Eqs. (3) and (4). Although the condition $\delta h(\rho=\rho_0)=0$ is not compatible with Eq. (3), it is best approached by the choice $c=\rho_0$, which also minimizes the gravitational potential energy.

In what follows we consider the elastic case first and then transpose our results to the viscous case. For inextensional elastic deformations, the energy functional reads

$$\begin{aligned} E[h+\delta h] &= \int_{\text{bubble}} d(\text{surface})(\text{gravitational energy} \\ &\quad + \text{bending energy}) \\ &= \int_R^{\rho_0}\rho d\rho\int_0^{2\pi} d\theta\sqrt{1+[\nabla[h+\delta h)]^2} \\ &\quad \{\,\mu g(h+\delta h) + \frac{K}{2}[\nabla^2(h+\delta h)]^2\}. \end{aligned} \qquad (5)$$

Here $K = Ye^3/12(1-\nu^2)$ is the effective rigidity, where Y is the Young modulus and ν the Poisson ratio. On substituting Eqs. (2–4) into Eq. (5) we obtain, to lowest order in the perturbation,

$$\begin{aligned} \delta E &\equiv E[h+\delta h] - E[h] \\ &= \frac{\pi}{2}K\varphi(\frac{\rho_0}{R})\sum_{n\geq 1}(\delta\beta_n)^2\{-\gamma R^3\psi(\frac{\rho_0}{R}) \\ &\quad + [1-\gamma R^3\psi(\frac{\rho_0}{R})]n^2 + n^4\} \\ &\equiv \sum_{n\geq 1}\delta E_n, \end{aligned} \qquad (6)$$

where

$$\gamma = \frac{\mu g}{\alpha K}, \quad \varphi\left(\frac{\rho_0}{R}\right) = \ln\left(\frac{\rho_0}{R}\right), \text{ and}$$

$$\psi\left(\frac{\rho_0}{R}\right) = \frac{\int_R^{\rho_0} d\rho\rho\,(\rho_0-\rho)}{R^3\ln(\rho_0/R)} = \frac{\frac{1}{3}-\frac{1}{2}\left(\frac{\rho_0}{R}\right)+\frac{1}{6}\left(\frac{\rho_0}{R}\right)^3}{\ln(\rho_0/R)}. \quad (7)$$

Here, we have used Eq. (4) to eliminate $\delta\alpha$, and the result is valid when $(\delta\beta_n)^2 \sim \alpha\delta\alpha \ll \alpha \ll 1$. $\gamma^{-1/3}$ is an intrinsic length scale, arising from the competiton between gravity and bending elasticity.

Each mode contributes an amount δE_n to the change in energy, and rippling occurs if $\delta E_n < 0$ for some integer. In general, $\delta E_n < 0$ for a range of different n's; the most negative variation corresponds to the maximally growing perturbation, and thus sets the wavelength of the instability. From Eqs. (6) and (7), we see that the instability is unexpectedly suppressed when $\gamma < \gamma_c = R_m^{-2}(\rho_0 - R_m)^{-1}$. Here, R_m maximizes $R^3\psi(\rho_0/R)$, and is calculated from $(\rho_0 - R_m)\ln(\rho_0/R_m) = R_m\psi(\rho_0/R_m)$. Furthermore, for a given bubble size ρ_0, rippling does not appear as long as $R < R_c(\mu, K, \rho_0)$, where R_c is defined by $R_c^3\psi(\rho_0/R_c) = \gamma^{-1}$. Azimuthal continuity near a small hole translates into short wavelength deformations, associated with a high (bending) cost. Equivalently, if $R < \gamma^{-1/3}$, one expects deformations close to the hole to be forbiddingly expensive. Finally, the onset of rippling also depends on the *ratio* ρ_0/R (as seen from the implicit definition of R_c). This is related to the fact that the wavelength of the deformation close to the hole is R/ρ_0 times smaller than at the base, implying a bending cost $(\rho_0/R)^2$ times larger, while the gain in gravitational potential energy is proportional to $(\rho_0 - R)$. Minimizing δE in Eq. (6) yields the number of ripples as

$$n^* = \mathrm{Int}\left\{\left[\frac{\mu g R^3}{K}\cdot\frac{1}{2\alpha}\psi\left(\frac{\rho_0}{R}\right)-\frac{1}{2}\right]^{1/2}\right\}, \quad (8)$$

where $\mathrm{Int}\{x\}$ is the integer closest to x. This relation improves on the estimate of Ref. [1], where the authors consider the short time elastic behavior, and establishes its domain of validity.

The above calculation amounts to a linear stability analysis involving the forces $F = -\delta E/\delta h$ derived from the energy functional of Eq. (5). This balance of forces for the elastic sheet differs from the equations of motion of the viscous sheet only in that the elastic modulus Y is replaced by the viscosity η and the height h is replaced by the transverse velocity dh/dt of the sheet [8]. Indeed, for short times after the viscous bubble begins to collapse, this can be obtained by integrating the Stokes equations through the thickness [11,8]. Using such a procedure, one can write the viscous resistance to bending as $\frac{\eta e^3}{4(1-\nu^2)}\frac{d(\text{curvature})}{dt}$ [8], so that the effective bending modulus of a liquid sheet is $K = K_l = \eta e^3/3\tau$ ($\nu = 1/2$ for an incompressible medium), where τ is a time scale associated with the falling velocity. Thus, all the conclusions of the stability analysis for the elastic sheet, and in particular the expression for the number of ripples (Eq. (8)), may be transposed to the case of the bubble modulo a certain time scale related to the gravity-induced velocity of the fluid. Comparing the nascent ripples' amplitude to the film thickness yields an estimate of this time scale as $(e/g)^{1/2}$. However, as the bubble continues to fall, this time scale may vary and so may the number of ripples. This last possibility is unlikely owing to the large forces required to introduce new ripples or remove existing ones.

In order to check our results against experiment, we visualized the bursting of silicone oil bubbles. Once the bubble is punctured with a sharp needle, its evolution is followed using a high-speed camera capable of recording up to 1000 frames per second. The resulting video is then analyzed to determine the radius ρ_0 of the bubble, the hole size R at which the ripples are first observed, along with the number of ripples n^*. As mentioned above, the hole expands very fast at first; by the time the pressure difference has equilibrated and the bubble begins to collapse, R is much larger than R_c. In order to compare the experiments with the theory, in which R enters as a parameter, the latter is measured at the onset of the instability for each given size of the bubble. In Fig. 2, we plot n^* as a function of ρ_0, which compares well with the theoretically predicted curve. Furthermore, the critical dependence of the rippling on the radius ρ_0 is qualitatively confirmed by the experiments which showed a supression of the instability for small bubbles.

We conclude with a discussion of possible refinements of the theory and their relation to the geometric nature of the problem. A more complete theory would incorporate a (flattened) hemisphere as the initial condition, rather than a cone. Also, while we argued that the inevitable stretching is limited to a negligible region, we have assumed that the latter is relegated to the lower edge of the bubble, disregarding the fact that the liquid is progressively drained out of the film by gravity so that the sheet is thinner around the hole and therefore more extensible (but also even more flexible) at the top than at the bottom. Though we expect, given the boundary conditions, that the stretching occurs quite generally near the base, improvements on the theory would be accompanied by the choice of more complicated ansatzes in Eqs. (1) and (2), and include a variable thickness $e(\rho)$; the corresponding calculations will

be reported elsewhere [11]. Yet, the strong geometrical constraints involved in the problem are suggestive of the robustness of the results. The question we have answered is akin to that of applying a curved surface unto a flat one in the most economical way, a problem which has taxed cartographers for many centuries and lies at the birth of differential geometry. It is also somewhat of an inverse counterpart to the problem of fitting a flat sheet to a three dimensional landscape, which has been studied in various contexts [12–15], and is an issue that still vexes fashion designers. The relevance of the geometrical constraints is manifest, for example, in the strong dependence of the rippling on the size of the opening, which is closely related to a well-known theorem due to Gauss [16], Jellett [17], and others, according to which (loosely put) a closed surface cannot be bent without being stretched, while an open surface can be bent inextensionally. Similarly, we find that a smaller hole implies a relatively stiffer bubble, and hampers the rippling. While the detailed form of the functions φ and ψ arise from the physical constraints and dynamics imposed by the the energy functional (or forces) and the various boundary conditions, the essence is in the geometry.

ACKNOWLEDGMENTS R.d.S. wishes to thank Georges Debrégeas for introducing him to the problem and sharing enthusiasm and insight. He is also very grateful to Professor Mehran Kardar for his precious guidance and comments. S.C. thanks Professor Gareth McKinley for his support. R.d.S. is supported by the NSF through Grant No. DMR-98-05833. S.C. is supported by the NASA through Grant No. NAG3-2155. L.M. is supported by the Sloan fund and the Karl van Tassel Chair at MIT.

[1] G. Debrégeas, P.-G. de Gennes, and F. Brochard-Wyart, Science **279**, 1704 (1998).
[2] D. Brush and B. Almroth, *Buckling of bars, plates and shells* (McGraw-Hill, New York, 1975).
[3] G. I. Taylor, *Proc. 12th Intl Congr. Appl. Mech.*, 382 (1969).
[4] L. Mahadevan, W. S. Ryu, and A. D. T. Samuel, Nature **392**, 140 (1998).
[5] G. Debrégeas, P. Martin, and F. Brochard-Wyart, Phys. Rev. Lett. **75**, 3886 (1995).
[6] L. D. Landau and E. M. Lifshitz, *Theory of Elasticity*, 3rd Edn. (Pergamon, New York, 1986).
[7] J. D. Buckmaster, A. Nachman, and L. Ting, J. Fluid Mech. **69**, 1 (1975).
[8] P. D. Howell, Eur. J. of App. Math. **7**, 321 (1996).
[9] A. E. H. Love, *A Treatise on the Mathematical Theory of Elasticity*, 4th Edn. (Dover, New York, 1944).
[10] Y. C. Fung and W. H. Wittrick, Q. J. Mech. App. Math. **8**, 191 (1955).
[11] R. da Silveira, S. Chaieb, and L. Mahadevan, in preparation.
[12] Y. Kantor, M. Kardar, and D. R. Nelson, Phys. Rev. Lett. **57**, 791 (1986).
[13] A. Lobkovksy, S. Gentges, H. Li, D. Morse and T. Witten, Science **270**, 1482 (1995).
[14] S. Chaïeb, F. Melo, and J.-C. Géminard, Phys. Rev. Lett. **80**, 2354 (1998).
[15] E. Cerda and L. Mahadevan, Phys. Rev. Lett. **80**, 2358 (1998).
[16] M. Spivak, *A Comprehensive Introduction to Differential Geometry*, vol. I, 2nd Edn. (Publish or Perish, 1979).
[17] J. H. Jellett, Dublin Roy. Irish Acad. Trans. **22** (1855).

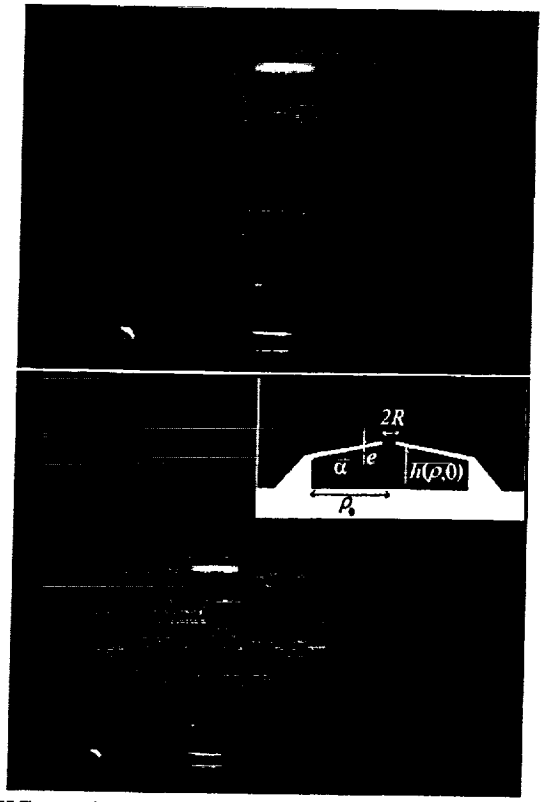

FIG. 1. Stroboscopic images of a collapsing liquid bubble of size is $\rho_0 = 1$mm and thickness $e \approx 100\mu$m. The silicone oil has viscosity $\eta = 10^3$Pa·s, surface tension $\sigma = 21$mN/m, and mass density 0.98g/cm^3. (a) 30ms after the film is punctured by a sharp needle, the bubble shows a retracting hole of radius $R = 1.4$mm at its apex, but no ripples yet. (b) 30ms later, the bubble loses its axisymmetric shape. The radius of the hole remains essentially constant, at $R = 1.6$mm, while the ripples grow. (The decrease in amplitude upon approaching the hole is noticeable.) The inset displays a schematic side view of the essentially conical deflating bubble at the onset of the instability, with the important quantities involved in the phenomenon. The extreme shallowness allows for a perturbative treatment in the slope α of the cone.

FIG. 2

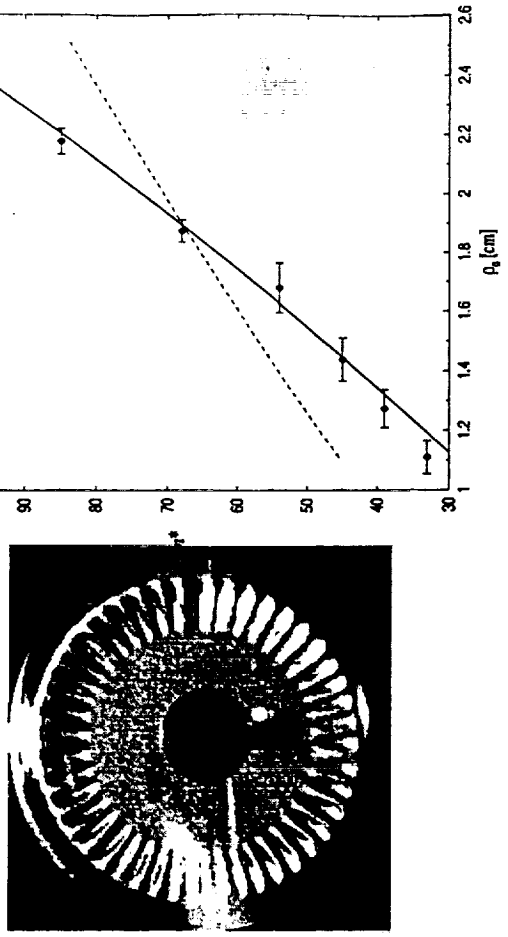

FIG. 2. Plot of the number of ripples n^* as a function of the bubble radius ρ_0, comparing the experimental measures (points) with the theoretical prediction (solid line). These data were gathered using solicone oil of viscosity $\eta = 600\text{Pa}\cdot\text{s}$ and bubbles of thickness $e \approx 30\mu\text{m}$. The errors in the measurement of ρ_0 arise from meniscus effects which are more important in smaller bubbles. The bursting time elapsed up to rippling is measured to be of order of 1 to 5 times $(e/g)^{1/2}$, consistent with our proposed mechanism for the formation of the corrugation. For each experimental realization, the ratio ρ_0/R was measured at the onset of the instability, and the corresponding dependence of R on ρ_0 was used to get a theoretical curve $n^* = n^*(\rho_0)$. The latter is plotted here for a slope $\alpha \approx 3°(\approx 0.05\text{rad})$ of the cone, consistent with our perturbative treatment, and in agreement with direct observation. The dashed line represents the best fit of the scaling form $n^* \sim \left(\mu g R^3/K\right)^{1/2}$ [1], where R is chosen as the relevant length scale. If R is replaced by ρ_0, the above expression for n^* may be closely fitted (up to an overall multiplicative factor) to our predicted curve, showing that the size of the bubble is the dominant length scale within the present experimental range and conditions. We also note that the predictions compare best with the experimental data for larger bubbles $(e/\rho_0 \ll 1)$, for which an inextensible model is better suited. The inset shows a top view of the fully developed ripples, from which n^* is measured.